

## Effects of the antitumoural dequalinium on NB4 and K562 human leukemia cell lines Mitochondrial implication in cell death

Eva Galeano<sup>a</sup>, Elena Nieto<sup>a</sup>, Ana Isabel García-Pérez<sup>a</sup>, M.Dolores Delgado<sup>b</sup>,  
Montserrat Pinilla<sup>a</sup>, Pilar Sancho<sup>a,\*</sup>

<sup>a</sup> Departamento de Bioquímica y Biología Molecular, Facultad de Medicina, Universidad de Alcalá, Alcalá de Henares, Madrid, Spain

<sup>b</sup> Grupo de Biología Molecular del Cáncer, Departamento de Biología Molecular y Unidad de Biomedicina-CSIC,  
Universidad de Cantabria, Santander, Spain

Received 16 February 2005; accepted 15 March 2005

Available online 12 May 2005

---

### Abstract

Dequalinium (DQA) is a delocalized lipophylic cation that selectively targets the mitochondria of carcinoma cells. However, the underlying mechanisms of DQA action are not yet well understood. We have studied the effects of DQA on two different leukemia cell lines: NB4, derived from acute promyelocytic leukemia, and K562, derived from chronic myeloid leukemia. We found that DQA displays differential cytotoxic activity in these cell lines. In NB4 cells, a low DQA concentration (2  $\mu$ M) induces a mixture of apoptosis and necrosis, whereas a high DQA concentration (20  $\mu$ M) induces mainly necrosis. However, K562 cell death was always by necrosis as the cells showed a resistance to apoptosis at all time-periods and DQA concentrations assayed. In both cell lines, the cell death seems to be mediated by alterations of mitochondrial function as evidenced by loss of mitochondrial transmembrane potential,  $O_2^{\bullet-}$  accumulation and ATP depletion. The current study improves the knowledge on DQA as a novel anticancer agent with a potential application in human acute promyelocytic leukemia chemotherapy.

© 2005 Elsevier Ltd. All rights reserved.

**Keywords:** Dequalinium; Leukemia; K562 cells; NB4 cells; Apoptosis; Necrosis; Mitochondria; Reactive oxygen species

---

### 1. Introduction

Most of the antitumour agents used in chemotherapy are aimed at inducing malignant cell death in order to eradicate the tumour, thus limiting its growth and spreading. However, the lack of specificity for tumour cells exhibited by these agents causes undesirable side effects that have led to the investigation of new therapeutic strategies designed to specifically target malignant cells and thus trigger selective cell destruction.

It is well established that the efficacy of conventional anti-tumour drugs is due to their ability to induce apoptosis [1–3].

Mitochondria are now known to play a critical role in initiating apoptotic cell death [4–6]. Thus, diverse stress stimuli induce mitochondrial changes, which result in the release of apoptogenic factors into the cytoplasm such as cytochrome *c*, clearly observed in the early phases of apoptosis. This is associated with changes in the mitochondrial ultra-structure, membrane permeability, transmembrane potential, and caspase activation [6–9].

Intriguingly, a wide variety of carcinoma cells exhibit increased accumulation and retention of delocalized lipophylic cations (DLCs) due to a higher negative mitochondrial transmembrane potential in tumour cells than in normal cells [10,11]. This behaviour provides an attractive basis for the use of DLCs in selective tumour cell eradication. Among the wide variety of DLCs, dequalinium (DQA, chemical

---

\* Corresponding author. Tel.: +34 91 8854581; fax: +34 91 8854585.

E-mail address: [pilar.sancho@uah.es](mailto:pilar.sancho@uah.es) (P. Sancho).

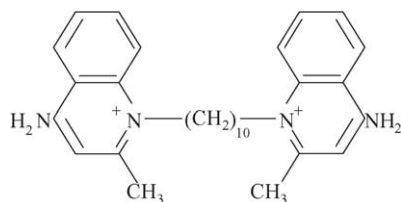


Fig. 1. Structure of DQA.

structure shown in Fig. 1) has been reported to display a potent anticancer activity in cells from different malignancies [12–15]. Most of the studies on DQA cytotoxicity have been performed in tumour cells of epithelial origin [16]. However, the effects of DQA on other cell types such as hematopoietic malignancies remain unknown.

The present work is aimed at analyzing the effects of DQA on two human leukemia cell lines: NB4, derived from acute promyelocytic leukemia, and K562, derived from chronic myeloid leukemia in blastic crisis. We have explored cell growth and metabolic activity as well as DQA-induced cell death via apoptosis or necrosis after DQA treatment. Although the molecular mechanisms underlying DQA-induced cell death are not well understood, several studies have related the antitumour effects of DQA to its accumulation in mitochondria [17–21]. Therefore, in the present study, DQA-induced leukemia cell death is analyzed in relation to mitochondrial function by studying the transmembrane potential, reactive oxygen species (ROS) production and ATP synthesis.

## 2. Materials and methods

### 2.1. DQA preparation

DQA was prepared as previously described [22,23]. Briefly, a 10 mM dequalinium chloride (Sigma Chemical Co., St. Louis, MO, MW 527.6) stock solution was prepared by dissolving an adequate amount of DQA in methanol in a round bottom flask. The organic solvent was removed with a rotary evaporator. The DQA-film obtained was resuspended in 5 mM HEPES, pH 7.4 and sonicated for 1 h. Finally, the sample was centrifuged ( $1000 \times g$ , 5 min) to remove metal particles from the probe as well as larger DQA aggregates. This procedure yielded an opaque solution of liposome-like DQA vesicles, which was then filtered using a  $0.2 \mu\text{M}$  filter. The DQA concentration was determined by fluorimetry (Perkin-Elmer LS-50 B Spectrofluorimeter, excitation  $\lambda = 335 \text{ nm}$ , emission  $\lambda = 360 \text{ nm}$ ). The DQA standard curve was found to be linear between 0.001 and 0.01 mM DQA ( $r^2 = 0.998$ ).

### 2.2. Cell cultures

NB4 and K562 leukemia cell lines were obtained from the American Type Culture Collection. Cells were grown

in RPMI 1640 medium (Gibco-Life Technologies, Scotland, UK) supplemented with 8% heat-inactivated fetal calf serum (FCS, Gibco-Life Technologies) and gentamycin ( $80 \mu\text{g/ml}$ ). Cells were seeded at a density of  $2\text{--}3 \times 10^5 \text{ cells/ml}$ . Cultures were maintained at  $37^\circ\text{C}$  in a humidified 5%  $\text{CO}_2$  atmosphere.

### 2.3. Cell growth and viability assays

Exponentially growing NB4 or K562 cell cultures ( $2\text{--}3 \times 10^5 \text{ cells/ml}$ ) were treated with increasing ( $0.5\text{--}20 \mu\text{M}$ ) DQA concentrations for either 24 or 48 h. When experiments were carried out in the presence of imatinib, a  $2 \mu\text{M}$  concentration was used [24]. Imatinib (STI571, Gleevec®) was kindly provided by Novartis Pharma AG (Basel, Switzerland). Cell density was measured with a Neubauer hemocytometer. Metabolic activity of the cells was assessed with a MTT kit (Roche Mannheim, Germany) to detect mitochondrial dehydrogenase activity. Viable cells, with functional mitochondria, were able to reduce the tetrazolium ring to a blue formazan product whereas dead cells remained uncolored. The  $\text{IC}_{50}$  is defined as the drug concentration that induced a 50% loss of metabolic activity.

### 2.4. Necrotic cell death evaluation

NB4 and K562 cell death by necrosis was determined by the loss of cell membrane integrity using either the trypan blue exclusion dye or propidium iodide (PI) free influx in non-permeabilized cells. For the trypan blue exclusion test, cells were incubated with 0.2% (w/v) trypan blue for 5 min and analyzed by microscopy (OLIMPUS BHT) using a Neubauer hemocytometer. Only clearly blue-stained cells were considered as necrotic. For the study of PI accumulation, cells were incubated with  $50 \mu\text{g/ml}$  of PI and the emitted fluorescence was analyzed by flow cytometry in a FACScan (Becton Dickinson, San Jose, CA) with an FL-2 detector (620 nm band pass filter). Under these conditions, necrotic cells are brightly stained by PI and appear as a peak at very high fluorescence values. Apoptotic cells appear as a dimly fluorescent population. Since apoptosis ultimately leads to a loss of plasma membrane integrity, the necrosis determined here includes the late stages of apoptosis.

### 2.5. Apoptotic cell death evaluation

The characteristic decrease in DNA content in the apoptotic process was analyzed by flow cytometry of permeabilized PI-stained cells. Samples containing  $3\text{--}5 \times 10^5 \text{ cells}$  were incubated with  $0.5 \text{ mg/ml}$  of RNase A for 30 min. Cells were then permeabilized with 0.1% nonidet P-40 and incubated with  $50 \mu\text{g/ml}$  of PI. Cell cycle analysis was carried out by flow cytometry (FL-2 detector in a linear mode) using the Cell Quest Pro software (Becton Dickinson, San Jose, CA). Permeabilization of cells causes the leakage of the cleaved low MW DNA fragments that are produced during apoptosis.

As a consequence, apoptotic cells are identified as a hypodiploid peak, while healthy cells generate a typical cell cycle histogram. Non-apoptotic, primary necrotic cells are generally found among the healthy ones.

In order to analyze the changes in nuclear morphology characteristic of apoptosis (chromatin condensation, cytoplasmic shrinkage, and apoptotic body formation), 4,6-diamino-2-phenylindole (DAPI, SERVA, Heidelberg, Germany) cell staining was performed. Samples containing  $0.5 \times 10^6$  cells were pelleted by centrifugation, washed in PBS, resuspended and mounted on glass slides and fixed with 70% (v/v) ethanol. Cells were stained with 1  $\mu\text{g}/\text{ml}$  of DAPI and 10  $\mu\text{g}/\text{ml}$  of sulforhodamine 101 (Molecular Probes, Eugene, OR) and analyzed by fluorescent microscopy (OLYMPUS BHT, attached with BH2-reflected light fluorescence illuminator). At least 200 cells were scored for each point.

Apoptosis was also assessed by the presence of internucleosomal DNA fragmentation (DNA laddering) after cell exposure to DQA. DNA was isolated from 3 to  $5 \times 10^5$  cells and analyzed (approximately 2  $\mu\text{g}$  DNA) by electrophoresis on a 1% agarose gel containing 0.1  $\mu\text{g}/\text{ml}$  of ethidium bromide, as previously described [25].

### 2.6. Caspase-3 activity

Samples containing  $10 \times 10^6$  cells were washed in PBS and resuspended in 100  $\mu\text{l}$  of ice-cold lysis buffer (50 mM Tris-HCl, pH 7.5; 0.03% (v/v) nonidet P-40, 1 mM dithiothreitol) for 30 min at 4 °C. Cell extracts were centrifuged ( $13,000 \times g$  for 15 min at 4 °C) and aliquots of the supernatants (20  $\mu\text{g}$  of proteins) were incubated for 30 min at 37 °C with 200  $\mu\text{M}$  of DEVD-pNA (Calbiochem, Germany) caspase-3 substrate in a final volume of 200  $\mu\text{l}$ . Enzymatic caspase activity was calculated from the increase of absorbance at 405 nm during 2 h. The activity data are expressed in relation to the control data.

### 2.7. Western blot analysis of PARP and PKC- $\delta$ cleavage

Cellular protein extracts (10  $\mu\text{g}$ ) were analyzed by immunoblot according to a standard procedure [26]. PKC- $\delta$  and PARP cleavage were detected with a rabbit anti-human PKC- $\delta$  or PARP polyclonal antibody (Santa Cruz Biotechnology Inc., Santa Cruz, CA), respectively. An anti-human actin monoclonal antibody (Oncogene, EMD Biosciences Inc., Germany) was used to assess equal protein loading in all lanes. The signal was developed using the ECL western blotting analysis system obtained from Amersham (England, UK).

### 2.8. Measurements of superoxide anion

The intracellular accumulation of superoxide anion ( $\text{O}_2^{\bullet-}$ ) was determined using the fluorescent probe (Molecular Probes, Eugene, OR) dihydroethidium (DHE) [27]. Cells

were incubated with 2  $\mu\text{M}$  of DHE during the last 15 min of the DQA treatment. The fluorescence intensity was measured by flow cytometry (FL-2, 620 nm band pass filter).

### 2.9. Measurement of intracellular ATP

The intracellular ATP content was estimated by a luciferin-luciferase bioluminescence assay using the assay kit CLSII (Roche Diagnostics, Barcelona, Spain). ATP concentrations were calculated from a log-log plot of an ATP standard curve (linear in the range of  $10^{-6}$  to  $10^{-11}$  M). Bioluminescence was measured in a Multilabel Wallac Counter (Victor<sup>2</sup> EG&G Wallac, Finland).

### 2.10. Measurement of mitochondrial transmembrane potential ( $\Delta\Psi_m$ )

Cells ( $0.5 \times 10^6$ ) were washed with PBS and incubated for 15 min at 37 °C with 1  $\mu\text{g}/\text{ml}$  of rhodamine 123 (Sigma Chemical Co., St. Louis, MO). After washing, the cells were resuspended in 0.5 ml of PBS and the fluorescence was measured by flow cytometry (FL-1 detector).

## 3. Results

### 3.1. Cytotoxic activity of DQA

In order to investigate the cytotoxic activity of DQA on the NB4 and K562 leukemia cell lines, a concentration- and time-response study was initially carried out. Cells were treated with increasing DQA concentrations (from 0.5 to 20  $\mu\text{M}$ ) for either 24 or 48 h. As shown in Fig. 2A, DQA decreased the NB4 and K562 cell density in a concentration- and time-dependent way. After a 24-h treatment, a slight decrease in cell density, as compared with untreated cells, was observed from 0.5 to 20  $\mu\text{M}$  DQA. Moreover, when the cell density was compared to cells at the start of the experiment, some cell death could be clearly observed in both cell lines, at the highest DQA concentration (20  $\mu\text{M}$ ). The increase in incubation time from 24 to 48 h enhances these DQA effects. In all cases, NB4 cells proved to be more sensitive to the cytotoxic effect of DQA than K562 cells.

Mitochondrial dehydrogenase activity in metabolically active cells growing in the above experimental conditions was determined by the MTT test. Fig. 2B shows a loss of metabolic activity that was DQA concentration- and time-dependent in both the leukemic cell lines. The  $\text{IC}_{50}$  was around 4  $\mu\text{M}$  for NB4 cells and 12  $\mu\text{M}$  for K562 cells, after 24 h. A longer 48 h-incubation period had a much more potent effect, decreasing the  $\text{IC}_{50}$  to 2 and 2.5  $\mu\text{M}$  for NB4 and K562 cells, respectively. These results imply a higher cytotoxic effect of DQA on NB4 than on the K562 cells. In addition, these results indicate that after 24 h, DQA is active at a concentration as low as 0.5  $\mu\text{M}$ , although these cells show major metabolic alterations from 2  $\mu\text{M}$  DQA onwards.

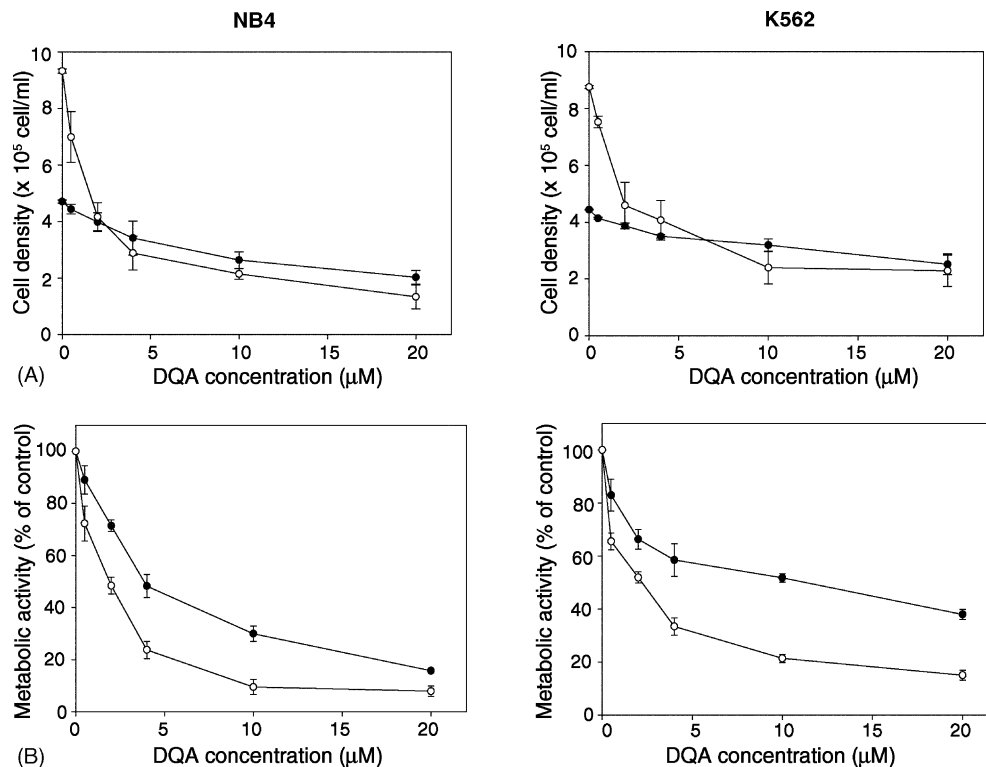


Fig. 2. (A) Cell density; and (B) metabolic activity of NB4 and K562 cells after 24 (●) or 48 (○) h of treatment with 0.5, 2, 4, 10 and 20 μM DQA. Cell density was scored in a cytometric chamber and metabolic activity was measured by the MTT test. Cells were seeded at a density of  $2\text{--}3 \times 10^5$  cells/ml. Data are presented as the mean  $\pm$  S.E.M., determined from three to six separate experiments.

### 3.2. DQA-induced cell death

The ability of DQA to induce NB4 or K562 cell death by necrosis or apoptosis was subsequently analyzed. The characteristic feature of the necrotic process such as the loss of cell membrane integrity was analyzed by both the trypan blue exclusion assay (Fig. 3A) and PI staining of cells (Fig. 3B). As shown in Fig. 3A, necrosis (>10%) was detected by trypan blue staining in NB4 cells from 10 μM DQA onwards, applied for 24 h or from 2 μM onwards, applied for 48 h. K562 cells treated with similar DQA concentrations showed necrosis (>10%) only at the highest DQA concentration, 20 μM, applied for 24 h or from 4 μM onwards applied for 48 h. Therefore, K562 cells undergo relatively less necrosis than NB4 cells.

Representative flow cytometry profiles of the PI uptake in control cells and cells incubated with 2 μM (low concentration) or 20 μM (high concentration) of DQA for 48 h are presented in Fig. 3B. These profiles indicate, once again, that a DQA concentration as low as 2 μM applied during 48 h induces some necrosis in NB4 but not in K562 cells. At the highest DQA concentration analyzed, significant necrosis was observed in both the cell lines, which was higher in NB4 than in K562 cells. The percentages of necrotic cells obtained by this method were similar to those observed by the trypan blue exclusion assay.

DQA-induced apoptosis was studied by cell cycle analysis obtained by flow cytometry after PI staining of previously permeabilized cells. Fig. 4A shows a representative example of the NB4 and K562 PI fluorescent profiles obtained from controls and cells incubated with 2 or 20 μM DQA for 48 h. The typical histogram with two well-defined peaks corresponding to the G<sub>0</sub>/G<sub>1</sub> and G<sub>2</sub>/M phases was clearly observed in control cells. The apoptosis percentage, obtained from cells in the sub-G<sub>0</sub>/G<sub>1</sub> regions at the different DQA concentrations and time-periods employed is shown in Fig. 4B. Apoptosis percentage was about 3% in either NB4 or K562 control cells. NB4 cells did not practically undergo apoptosis after 24 h at any DQA concentrations, while apoptosis began at 0.5 μM and became evident between 2 and 10 μM DQA, after 48 h of DQA treatment. Under similar experimental conditions no apoptosis (<7%) was detected in K562 cells. The dramatic difference in the cell cycle profile of K562 cells treated with 20 μM DQA compared to control cells (Fig. 4A) is striking. This indicates cell cycle arrest of K562, without accumulation in any specific phase of the cycle, which is in agreement with the proliferation arrest shown in Fig. 2A.

K562 cells are known to express the fusion protein Bcr-Abl that provides continuous cell survival signalling [24,28]. To determine whether Bcr-Abl was responsible for the resistance to apoptosis observed in K562 cells, experiments in the presence of imatinib, a potent inhibitor of Bcr-Abl kinase

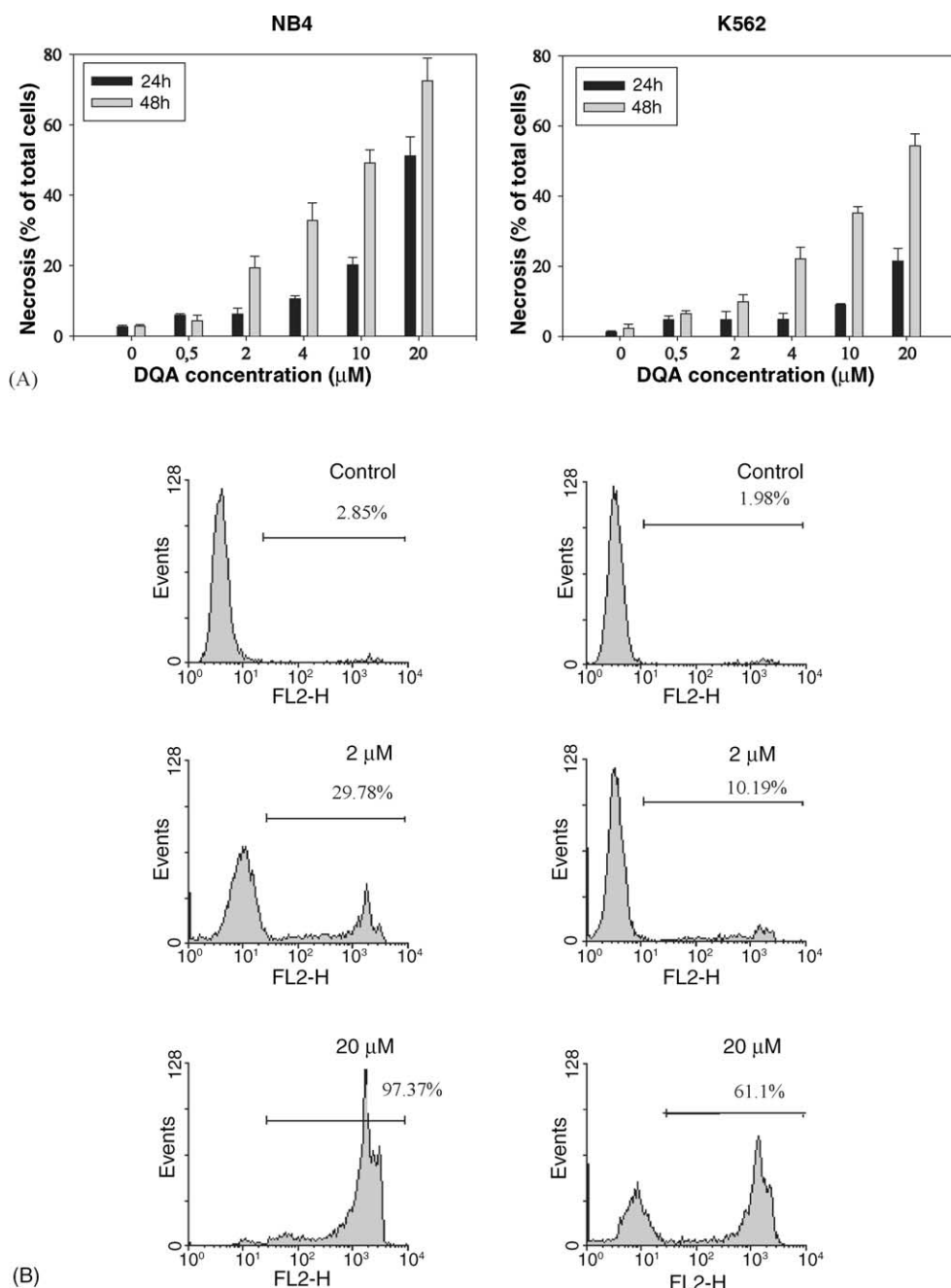


Fig. 3. Effect of DQA treatment on necrotic cell death in NB4 and K562 cells. (A) Necrosis frequency of cells treated for the indicated time-periods and with the indicated concentrations of DQA as measured by trypan blue. Data are presented as the mean  $\pm$  S.E.M., determined from three to six separate experiments. (B) Representative flow cytometric profiles of untreated (control) cells or cells treated for 48 h with the indicated DQA concentrations, as evaluated by PI accumulation in non-permeabilized cells; the percentage of necrosis is shown in each profile.

activity, were carried out. Cells were incubated for 48 h with both DQA (2  $\mu\text{M}$ ) and imatinib (2  $\mu\text{M}$ ). The results obtained show that in the presence of imatinib, DQA was able to induce apoptosis (around 20%) in K562 cells. Under similar experimental conditions, DQA did not increase the apoptosis in NB4 cells observed when incubated with DQA alone. These results indicate that inhibition of Bcr-Abl kinase activity by imatinib may sensitize K562 cells to apoptosis induced by DQA.

### 3.3. Studies on apoptotic events

Some characteristic features of apoptotic cell death were then comparatively analyzed in NB4 and K562 cells treated with the two lowest DQA concentrations, 0.5 and 2  $\mu\text{M}$ , for 48 h. As determined by DAPI staining, DQA-treated NB4 cells displayed typical apoptotic nuclear morphological changes, such as chromatin condensation and apoptotic body formation. Fig. 5A shows a representative picture

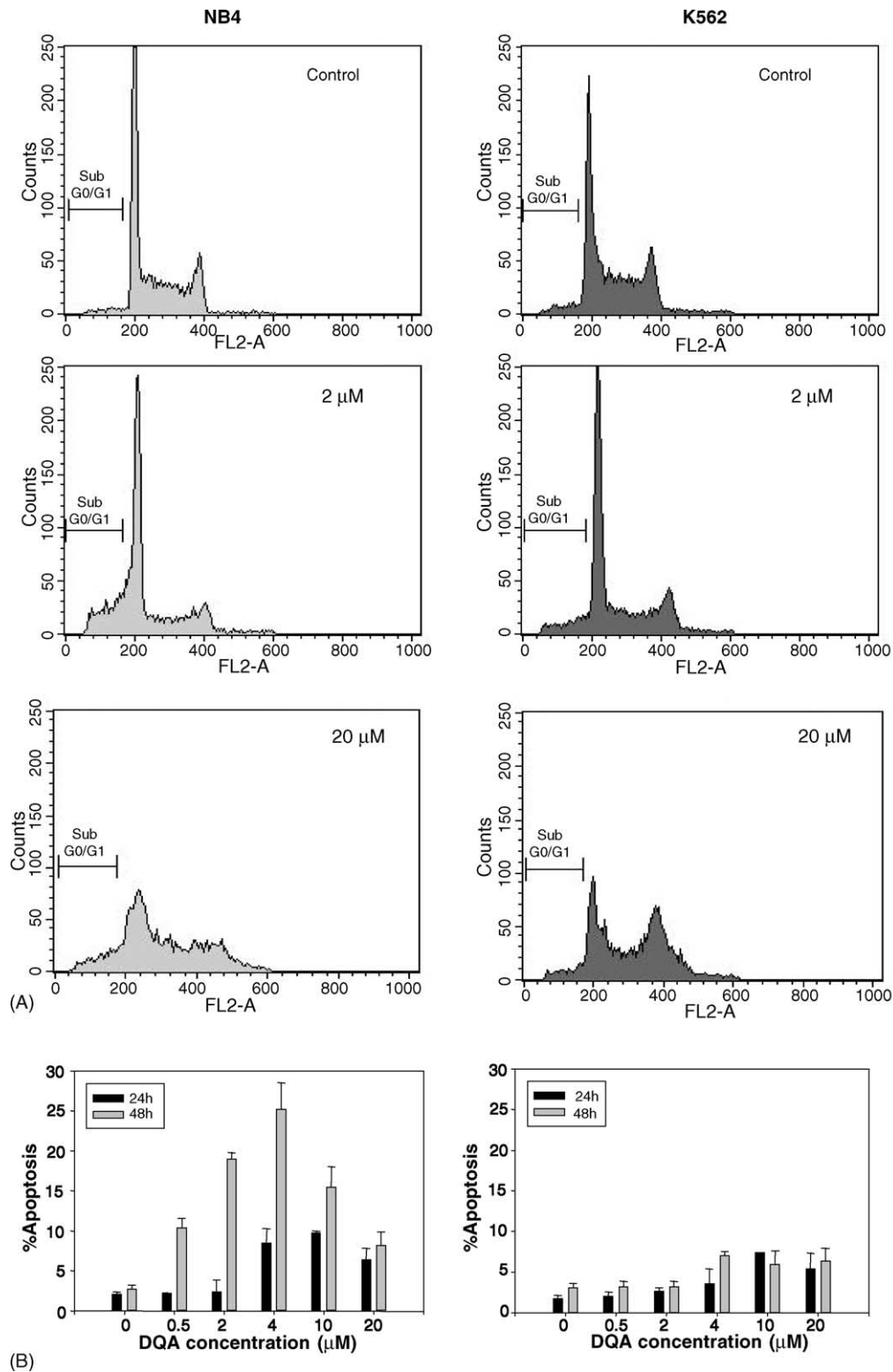


Fig. 4. Effect of DQA treatment on apoptotic cell death in NB4 and K562 cells. (A) Representative cell cycle distribution profiles of untreated (control) cells or cells treated for 48 h with the indicated DQA concentrations, as measured by flow cytometry after cell permeabilization and PI staining. (B) Frequency of apoptosis after a 24- or 48-h incubation with the indicated DQA concentrations. Data were obtained from the corresponding sub-G<sub>0</sub>/G<sub>1</sub> regions and presented as the mean  $\pm$  S.E.M. of three to six separate experiments.



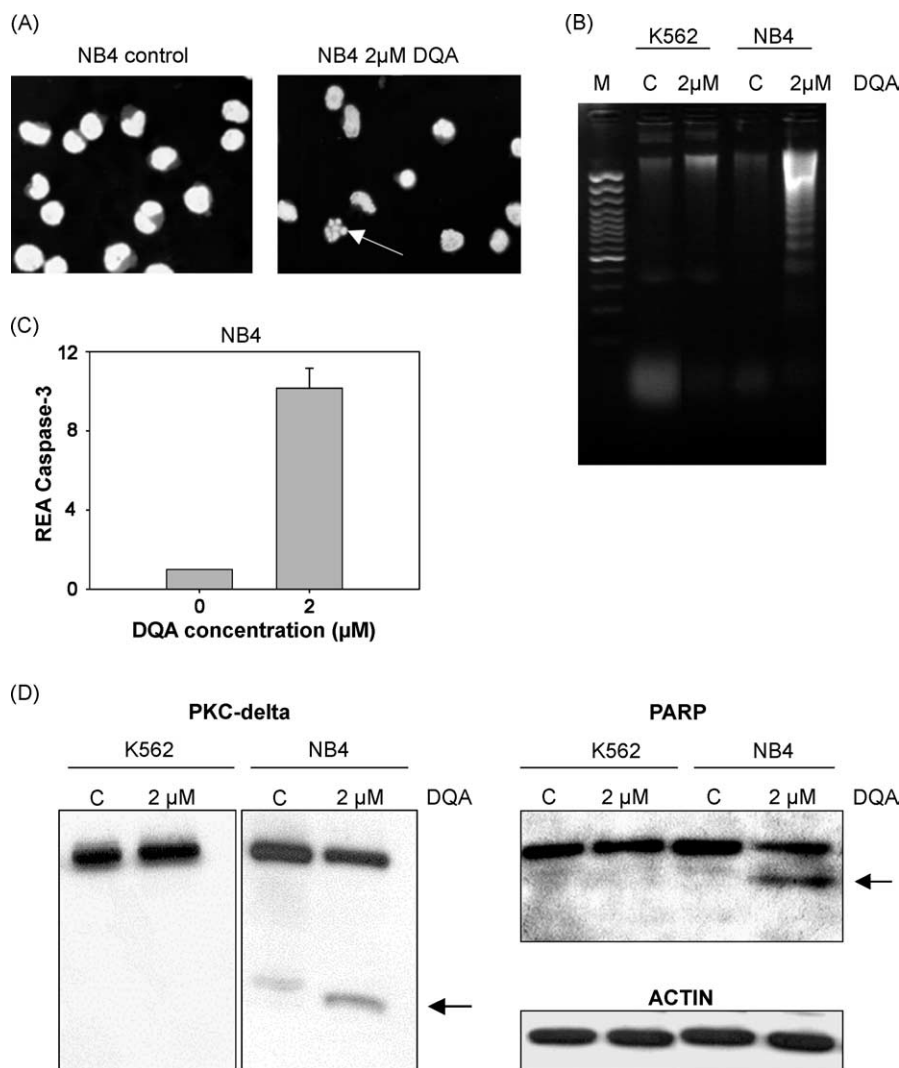


Fig. 5. Apoptotic intracellular events in NB4 cells treated for 48 h with 2  $\mu$ M DQA. (A) DAPI stain; the arrow indicates a typical apoptotic cell. (B) Genomic DNA fragmentation assay of untreated cells (lane C) or cells treated with DQA as indicated. Lane M shows the DNA size markers. (C) Relative caspase-3 enzymatic activity (REA) with respect to the control. Data are presented as the mean  $\pm$  S.E.M., determined from six separate experiments. (D) DQA-induced PKC- $\delta$  and PARP cleavage analyzed by Western blot. The arrows indicate the position of the PKC- $\delta$  and PARP proteolytic fragments. Anti-human actin monoclonal antibody was used to assess equal protein loading in all the lanes.

obtained with 2  $\mu$ M DQA. Under these conditions,  $17.3 \pm 2.5\%$  of cells showed apoptotic morphology. Such a percentage is comparable to that obtained by flow cytometry from sub-G<sub>0</sub>/G<sub>1</sub> phase analysis (Fig. 4A). In contrast, K562 cells displayed no morphological signs of apoptosis (results not shown). The internucleosomal DNA fragmentation studied by agarose gel electrophoresis confirmed, through the typical DNA laddering, the presence of apoptosis in NB4 but not in K562 cells treated with DQA (Fig. 5B).

Another typical event for apoptotic cell death is activation of the caspase cascade. The activity of caspase-3, a critical down-stream effector of apoptosis, was markedly increased in NB4 cells treated with 2  $\mu$ M DQA for 48 h as compared to control cells (Fig. 5C). As expected by the absence of apoptosis in K562 cells, we could not detect any caspase-3 activity in these cells after DQA treatment (results not shown). Caspase

activation in NB4 cells was confirmed by immunoblotting. Two known substrates for caspase-3 are the pro-apoptotic protein PKC- $\delta$  and the DNA-binding protein PARP involved in DNA repair [29]. A cleaved 40 kDa fragment from PKC- $\delta$  and a cleaved 89 kDa fragment from PARP were detected in NB4 but not in control or K562 cell extracts after DQA treatment (Fig. 5D). Although a slight PKC- $\delta$  cleavage was observed in control cells, the 40 kDa fragment was clearly increased at the same time that the non-fragmented band was decreased in DQA-treated cells with respect to the controls. These results indicate that DQA induces typical caspase-3 mediated apoptosis in NB4 cells when treated with a DQA concentration equal to or greater than 2  $\mu$ M for 48 h.

In summary, we can highlight that low DQA concentrations, from 0.5 to 2  $\mu$ M, applied for 48 h, induces a mixture of apoptosis and some necrosis in NB4 cells while a high

20  $\mu\text{M}$  concentration induces mainly necrosis in both NB4 and K562 cell populations.

### 3.4. Studies on mitochondrial function

In order to determine the mechanism underlying the cytotoxicity of DQA in NB4 and K562 cells, we next investigated mitochondrial function. Mitochondrial DQA accumulation is likely to affect relevant cellular processes such as redox and energetic balance or transmembrane potential, all of which lead to cell death. Selection of the cell death pathway has been proposed to depend on both ROS production and ATP synthesis, which are tightly regulated by

the mitochondrial transmembrane potential [7]. The experimental conditions selected for these studies were 48 h of treatment with three DQA concentrations: 0.5  $\mu\text{M}$ , the concentration at which apoptosis is initiated in NB4 cells; 2  $\mu\text{M}$ , which induces a mixture of apoptosis–necrosis in NB4 cells; and 20  $\mu\text{M}$ , which induces necrosis in both cell lines (see Figs. 3A and 4B).

The mitochondrial transmembrane potential ( $\Delta\psi_m$ ) was investigated with the fluorescent probe Rhodamine 123 (Rh123). Representative flow cytometry histograms are shown in Fig. 6A. The average medians from fluorescence histograms appear in Fig. 6C. Both NB4 and K562 cells undergo a progressive depolarisation from 0.5 to 20  $\mu\text{M}$  DQA,

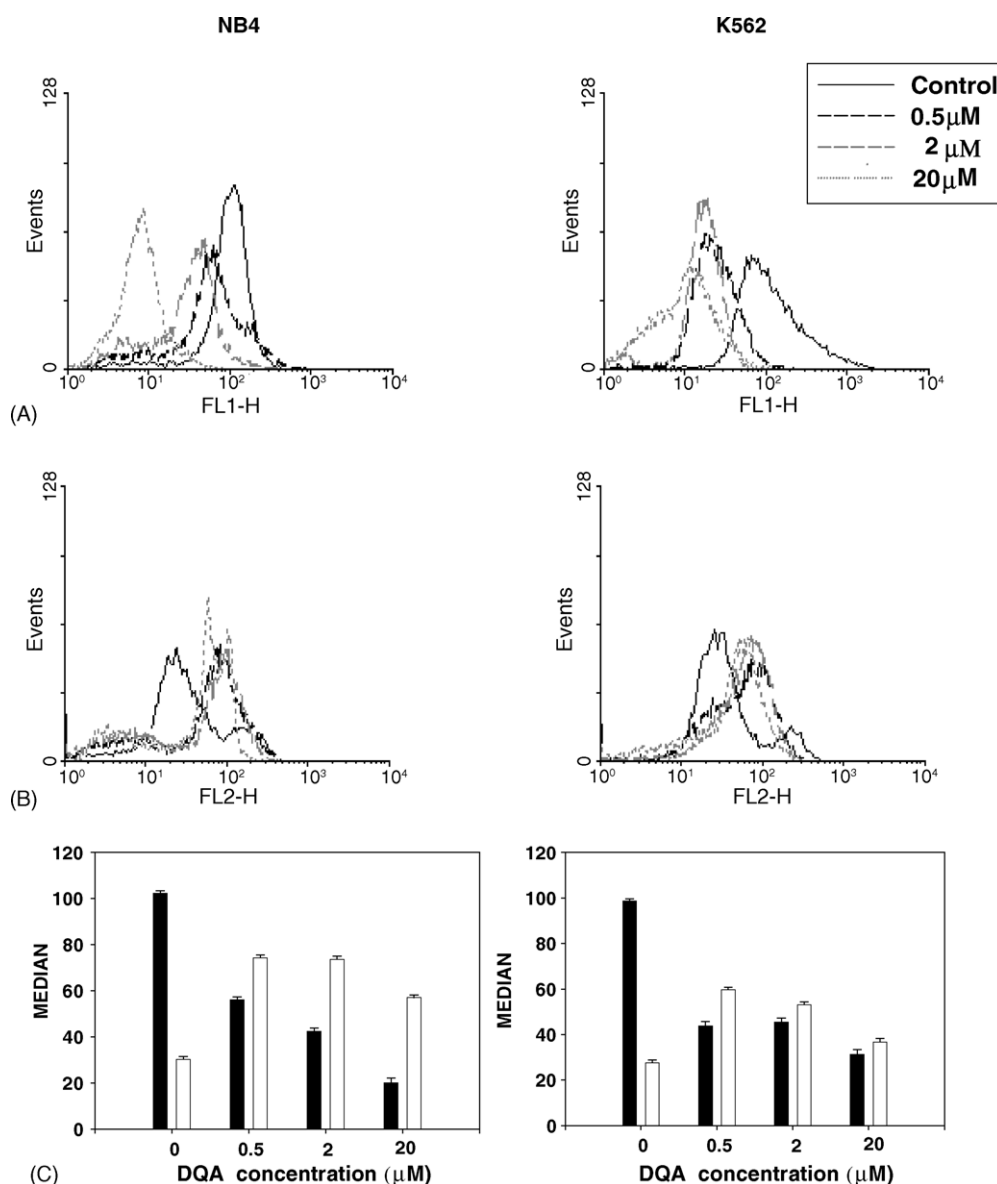


Fig. 6. Effect of DQA on mitochondrial function in NB4 and K562 cells treated for 48 h with 0.5, 2 and 20  $\mu\text{M}$  DQA. (A) Median of mitochondrial transmembrane potential ( $\Delta\psi_m$ ) as determined by changes in fluorescence upon rhodamine 123 loading. (B) Median of DHE-derived fluorescence, as indicative of radical superoxide production. (C) Average medians from fluorescence histograms of Rhodamine 123 (■) and DHE (□). Data are presented as the geometric mean (antilogarithm of the medians logarithm)  $\pm$  S.D. from fluorescence histograms from three to six separate experiments.



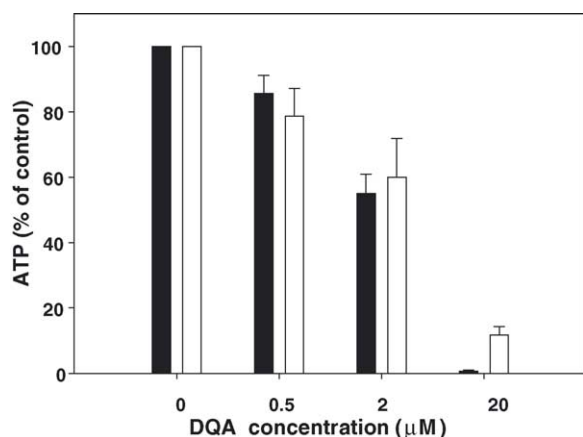


Fig. 7. ATP depletion in NB4 (■) and K562 (□) cells treated for 48 h with 0.5, 2 and 20  $\mu$ M DQA, as measured by a luciferin–luciferase bioluminescence assay. Data are presented as the mean  $\pm$  S.D. of at least three different experiments.

which is higher in NB4 cells at 20  $\mu$ M DQA. ROS generation was studied by measuring the DHE-derived fluorescence by flow cytometry, as indicative of the  $O_2^{\bullet-}$  levels. Representative flow cytometry histograms are shown in Fig. 6B. The average medians from fluorescence histograms appear in Fig. 6C. As evidenced by the right-shift of the DHE fluorescent signal with respect to the control signal, DQA induces  $O_2^{\bullet-}$  overproduction in both NB4 and K562 cells, even at the lowest concentration (0.5  $\mu$ M) employed. The  $O_2^{\bullet-}$  increase was more pronounced in NB4 cells than in K562 cells.

The effect of DQA on intracellular ATP content is shown in Fig. 7. A low DQA concentration of 0.5  $\mu$ M is enough to interfere with ATP synthesis in NB4 and K562 cells. An increased concentration of 2  $\mu$ M induces ATP depletion in both the cell lines, with slightly more pronounced effects in NB4 cells. Twenty micromolar DQA practically depleted ATP levels in both the NB4 and K562 cell lines. These results indicate an inhibitory effect of DQA on ATP synthesis in both the cell lines.

#### 4. Discussion

The major aim of this study was to investigate the molecular events underlying DQA cytotoxicity in NB4 and K562 leukemic cell lines derived from acute promyelocytic leukemia or from chronic myeloid leukemia, respectively. We demonstrate that DQA induces a progressive concentration- and time-dependent cytotoxic activity in both NB4 and K562 cell lines. These effects were more pronounced in NB4 cells and could be observed at the lowest concentration (0.5  $\mu$ M DQA) applied for 24 h.

Previous studies attribute to DQA different degrees of cytotoxicity depending on the cell type. DQA cytotoxicity is higher in cultured rat neurons [15] or P388 murine leukemic cells [30] than in the HeLa human cervical carcinoma cells [20] or NB4 and K562 human leukemic cells (present re-

sults). The mechanisms underlying the cytotoxic effects of DQA as well as the particular cellular response seems to be associated with changes in mitochondrial transmembrane potential of either tumour cells (in relation to normal cells) or with the different cell stages (for example, during neuronal maturation). Therefore, our aim was to elucidate the molecular events of DQA cytotoxicity in NB4 and K562 human leukemic cell lines in an attempt to take the advantage of its use for therapy of these malignancies.

We first investigated the implication of necrotic or apoptotic processes in cell death. The results indicate that the DQA-induced cell death was cell type-, time- and DQA concentration-dependent. After 48 h, low DQA concentrations induce apoptosis and some necrosis in NB4 cells whereas high concentrations induce necrosis in both cell populations. We observed an absence of apoptosis in K562 cells at all DQA concentrations analyzed, which was consistent with previous studies reporting a resistance of these cells to apoptosis [29,31–34]. K562 cells, derived from chronic myeloid leukemia, are deficient in the pro-apoptotic protein p53 and express the fusion protein Bcr-Abl kinase that provides continuous cell survival signaling. The apoptotic resistance of K562 cells has been shown to be overcome by treatment with drugs such as etoposide [29], cepharanthine [35],  $As_2O_3$  [36] or imatinib (STI 571) [37]. These drugs are able to induce apoptosis via different mechanisms including down-regulation of Bcr-Abl expression or inactivation of the tyrosine kinase activity of Bcr-Abl. In our hands, the apoptosis resistance of K562 cells treated with DQA was overcome by the kinase inhibitor imatinib. Therefore, Bcr-Abl kinase activity seems to be implicated in K562 cell survival signalling and in the resistance to DQA-induced apoptotic effects. We then carried out a study on mitochondrial function in both NB4 and K562 cell lines, using the latter as a negative control of apoptosis.

Two major apoptosis pathways (a receptor-mediated and a mitochondrial pathway) have been described in mammalian cells. Since DQA accumulates in the mitochondria [10], we searched for the mitochondrial implication in DQA-induced cytotoxicity. In both cell lines, we found that DQA induces a decrease in  $\Delta\Psi_m$ , an overproduction of  $O_2^{\bullet-}$  and ATP depletion effects, which were more pronounced in NB4 cells. These results indicate a mitochondrial dysfunction in both NB4 and K562 cell lines, mainly in NB4, in agreement with the higher cytotoxicity shown by these cells. This finding, together with caspase-3 activation, led us to suggest a mitochondrial implication in DQA-induced apoptosis observed in NB4 cells. Although the mitochondria of K562 are also affected by DQA, the cell resistance to apoptosis would trigger cell death by necrosis.

NB4 cells begin to show apoptosis at a DQA concentration as low as 0.5  $\mu$ M, although cytotoxicity and ATP depletion are low at this concentration. This apoptosis seems to be associated with the increase in  $O_2^{\bullet-}$  production observed. The increase in DQA concentration to 2  $\mu$ M not only increases the apoptosis percentage in NB4 cells but also induces necrosis.

This higher percentage of apoptosis and necrosis is associated with a high  $O_2^{\bullet-}$  production together with a significant ATP depletion. The higher the DQA concentration, the higher the necrotic cell death, being the ATP lost the more responsible for committing cells to necrosis. Thus, the results suggest that NB4 cell death is mediated by a ROS- and ATP-dependent mechanism. ROS accumulation induces cell death either by apoptosis, when ATP is sufficient for cell metabolism or by necrosis when ATP is significantly depleted.

ROS generation has been associated to cell damage. When an electron escapes from the electron transport chain, it may react with molecular oxygen and form  $O_2^{\bullet-}$ , which can oxidise important cellular components. Although ROS participate in normal cell signalling processes, a high ROS production causes an oxidative cell injury that has been associated to both human diseases [38–43] and cell death [7]. Our findings in leukemic cells are consistent with the hypothesis that ROS overproduction, as a consequence of a disturbance in mitochondrial functions, is responsible for DQA-induced cell death. In this regard, the redox sensitive JNK/SAPK signalling pathway [44] might be implicated. Since leukemia cells, like other cancer cells, are under an increased oxidative stress [7], the ROS overproduction should provide a unique advantage for killing these malignant cells. Thus, the ability of DQA to accumulate in the mitochondria and enhance ROS production gains relevance in relation to the cancer chemotherapy.

Similar effects as those observed in NB4 cells treated with 2  $\mu$ M DQA have been previously reported in other cell types. In this regard, Chan and Lin-Shiau [15] demonstrated that 0.46  $\mu$ M DQA induces cell death, partly mediated by apoptotic and necrotic processes, in primary neuronal cultures. An important ATP depletion (about 50%) at an early stage of DQA treatment is proposed to be responsible for the apoptosis–necrosis conversion. These findings have also been associated to an overproduction of  $H_2O_2$ , which is related to neurodegeneration [15]. Although we failed to detect  $H_2O_2$  overproduction in NB4 and K562 cells (results not shown), we detected a significant increase in  $O_2^{\bullet-}$ , the  $H_2O_2$  precursor, as compared to controls. Because oxidative stress is dependent on the dynamic balance between ROS generation and elimination, further studies will be focused on the possible implication of other ROS, such as  $H_2O_2$ , as well as on the cell antioxidant capacity.

On the other hand, it is well established that intracellular ATP levels are an important factor in determining the cell death mode, by necrosis or apoptosis [45–47]. Cells are committed to necrosis when ATP depletion prevents them from entering apoptosis [42]. The observed ATP depletion in NB4 and K562 cells induced by DQA could be related to the  $F_1$ -ATPase inhibition by DQA reported in bovine heart mitochondria [19]. It is feasible that DQA accumulates in the mitochondrial membrane, dissipating the proton gradient ( $\Delta\Psi_m$ ) and uncoupling oxidative phosphorylation. This can account for both the increased  $O_2^{\bullet-}$  production and decreased ATP synthesis detected. Thus, the lower the DQA

accumulation the lower the cytotoxicity. Differences in mitochondrial DQA accumulation between different cell types could be an attractive basis for searching a selective therapy.

In conclusion, we demonstrate that DQA displays differential cytotoxic activity in NB4 and K562 leukemia cell lines. The NB4 cell death in response to relatively low DQA concentrations occurs mainly through a mixture of apoptotic–necrotic processes and involves the activation of caspase-3, whereas high DQA concentrations induce necrotic cell death. K562 cells proved to be resistant to the apoptosis-inducing DQA treatment. Our results strongly suggest that K562 cells died mainly by necrosis. However, we cannot rule out the possibility that autophagy, which has been suggested as other mechanism for non-apoptotic death [48,49], could be taking place. DQA-induced NB4 and K562 cell death seems to be mediated by mitochondrial alterations, including loss of mitochondrial transmembrane potential,  $O_2^{\bullet-}$  accumulation and ATP depletion as notable intracellular events. This study emphasizes the importance of DQA as a selective and potential antileukemic agent, and encourages the performance of further studies in order to obtain a deeper knowledge on its action mechanism in cell death in order to improve the clinical outcomes.

## Acknowledgements

Eva Galeano and Elena Nieto contributed equally to this work. This work was supported by the Comunidad Autónoma de Madrid (CAM) and Fondo de Investigaciones Sanitarias (FIS). We thank Lilian Puebla, from the University of Alcalá, for linguistic assistance.

## References

- [1] Makin G. Targeting apoptosis in cancer chemotherapy. *Expert Opin Ther Targets* 2002;6:73–84.
- [2] Brady H. Apoptosis and leukaemia. *Br J Haematol* 2003;123:577–85.
- [3] Makin G, Dive C. Recent advances in understanding apoptosis: new therapeutic opportunities in cancer chemotherapy. *Trends Mol Med* 2003;9:251–5.
- [4] Jiang X, Wang X. cytochrome *c*-mediated apoptosis. *Annu Rev Biochem* 2004;73:87–106.
- [5] Preston TJ, Abadi A, Wilson L, Singh G. Mitochondrial contributions to cancer cell physiology: potential for drug development. *Adv Drug Deliv Rev* 2001;49:45–61.
- [6] Körper S, Nolte F, Thiel E, Schrezenmeier H, Rojewski M. The role of mitochondrial targeting in arsenic trioxide-induced apoptosis in myeloid cell lines. *Br J Haematol* 2004;124:186–9.
- [7] Pelicano H, Carney D, Huang P. ROS stress in cancer cells and therapeutic implications. *Drug Resis Updat* 2004;7:97–110.
- [8] Kluck RM, Bossy-Wetzel E, Green DR, Newmeyer DD. The release of cytochrome *c* from mitochondria: a primary site for Bcl-2 regulation of apoptosis Science (Washington DC). 1997;275:1132–1136.
- [9] Adrain C, Martin SI. The mitochondrial apoptosome: a killer unleashed by the cytochrome seas. *Trends Biochem Sci* 2001;26:390–7.
- [10] Modica-Napolitano JS, Aprile JR. Delocalized lipophilic cations selectively target the mitochondria of carcinoma cells. *Adv Drug Deliv Rev* 2001;49:63–70.

- [11] Chen LB. Mitochondrial membrane potential in living cells. *Annu Rev Cell Dev Biol* 1988;4:155–81.
- [12] Weissig V, Lizano C, Torchilin V. Micellar delivery system for dequalinium—a lipophilic cationic drug with anticarcinoma activity. *J Liposome Res* 1998;8:391–400.
- [13] Helige C, Smolle J, Zellnig G, Fink-Puches R, Kerl H, Tritthart HA. Effect of dequalinium on K1735-M2 melanoma cell growth, directional migration and invasion in vitro. *Eur J Cancer* 1992;29A:124–8.
- [14] Abdul M, Hoosein N. Expression and activity of potassium ion channels in human prostate cancer. *Cancer Lett* 2002;186:99–105.
- [15] Chan CF, Lin-Shiau SY. Suramin prevents cerebellar granule cell death induced by dequalinium. *Neurochem Int* 2001;38:135–43.
- [16] Modica-Napolitano JS, Nalbandian R, Kidd ME, Nalbandian A, Nguyen CC. The selective in vitro cytotoxicity of carcinoma cells by AZT is enhanced by concurrent treatment with delocalized lipophilic cations. *Cancer Lett* 2003;198:59–68.
- [17] Weiss MJ, Wong JR, Ha CS, Bleday R, Salem RR, Steele Jr GD, et al. Dequalinium, a topical antimicrobial agent, displays anticarcinoma activity based on selective mitochondrial accumulation. *Proc Natl Acad Sci USA* 1987;84:5444–8.
- [18] Christman JE, Miller DS, Coward P, Smith LH, Teng N. Study of the selective cytotoxic properties of cationic, lipophilic mitochondrial-specific compounds in gynecologic malignancies. *Gynecol Oncol* 1990;39:72–9.
- [19] Zhuo S, Paik SR, Register JA, Allison WS. Photoinactivation of the bovine heart mitochondrial FI-ATPase by [<sup>14</sup>C]dequalinium cross-links phenylalanine-403 or phenylalanine-406 of an alpha subunit to a site or sites contained within residues 44 0–459 of a beta subunit. *Biochem* 1993;32:2219–27.
- [20] Schneider KR, Ammini CV, Rowe TC. Dequalinium induces a selective depletion of mitochondrial DNA from HeLa human cervical carcinoma cells. *Exp Cell Res* 1998;245:137–45.
- [21] Weissig V, Torchilin VP. Towards mitochondria gen therapy: DQAsomes as a strategy. *J Drug Target* 2001;9:1–13.
- [22] Lizano C, Weissig V, Torchilin VP, Sancho P, García-Pérez AI, Pinilla M. In vivo biodistribution of erythrocytes and polyethyleneglycol-phosphatidylethanolamine micelles carrying the antitumour agent dequalinium. *Eur J Pharm Biopharm* 2003;56:153–7.
- [23] Weissig V, Lasch J, Erdos G, Meyer HW, Roweand Tc, Hughes J, et al. A novel potential drug and gen delivery system made from dequalinium. *Pharm Res* 1998;15:334–7.
- [24] Gomez-Casares MT, Vaqué JP, Lemes A, Molero T, Delgado MD. León J. c-myc expression in cell lines derived from chronic myeloid leukaemia. *Haematologica* 2004;89:241–3.
- [25] Cañelles M, Delgado MD, Hyland KM, Lerga A, Richard C, Dang CV, et al. Max and inhibitory c-Myc mutants induce erythroid differentiation and resistance to apoptosis in human myeloid leukemia cells. *Oncogene* 1997;14:1315–27.
- [26] Sambrook J, Russell DW. *Molecular, Cloning. A laboratory manual*. New York: Cold Spring Harbor Laboratory Press; 2001.
- [27] Curtin JF, Donovan M, Cotter TG. Regulation and measurement of oxidative stress in apoptosis. *J Immunol Methods* 2002;265:49–72.
- [28] Goldman JM, Melo JV. Chronic myeloid leukemia – advances in biology and new approaches to treatment. *N Engl J Med* 2003;349:1451–64.
- [29] Martins LM, Mesner PW, Kottke TJ, Basi GS, Sinha S, Tung JS, et al. Comparison of caspase activation and subcellular localization in HL-60 and K562 cells undergoing etoposide-induced apoptosis. *Blood* 1997;90:4283–96.
- [30] Hait WN, Pierson NR. Comparison of the efficacy of a phenothiazine and a bisquinaldinium calmodulin antagonist against multidrug-resistant P388 cell lines. *Cancer Res* 1990;50:1165–9.
- [31] Konopka JB, Watanabe SM, Witte ON. An alteration of the human c-abl protein in K562 leukemia cells unmasks associated tyrosine kinase activity. *Cell* 1984;37:1035–1042.
- [32] Law JC, Ritke MK, Yalowich JC, Leder GH, Ferrell RE. Mutational inactivation of the *p53* gene in the human erythroid leukemic K562 cell line. *Leuk Res* 1993;17:1045–50.
- [33] McGahon A, Bissonnette R, Schmitt M, Cotter KM, Green DR, Cotter TG. BCR-ABL maintains resistance of chronic myelogenous leukemia cells to apoptotic cell death. *Blood* 1994;83:1179–87.
- [34] Ceballos E, Delgado MD, Gutierrez P, Richard C, Muller D, Eilers M, et al. c-Myc antagonizes the effect of *p53* on apoptosis and p21WAF1 transactivation in K562 leukemia cells. *Oncogene* 2000;19:2194–204.
- [35] Wu J, Suzuki H, Zhou YW, Liu W, Yoshihara M, Kato M, et al. Cepharanthine activates caspases and induces apoptosis in Jurkat and K562 human leukemia cell lines. *Cell Biochem* 2001;82:200–14.
- [36] Perkins C, Kim CN, Fang G, Bhalla KN. Arsenic induces apoptosis of multidrug-resistant human myeloid leukemia cells that express Bcr-Abl or overexpress MDR, MRP, Bcl-2, or Bcl-x(L). *Blood* 2000;95:1014–22.
- [37] Fang G, Kim CN, Perkins CL, Ramadevi N, Winton E, Wittmann S, et al. CGP57148B (STI-571) induces differentiation and apoptosis and sensitizes Bcr-Abl-positive human leukemia cells to apoptosis due to antileukemic drugs. *Blood* 2000;96:2246–53.
- [38] Zhou Y, Hileman EO, Plunkett W, Keating MJ, Huang P. Free radical stress in chronic lymphocytic leukemia cells and its role in cellular sensitivity to ROS-generating anticancer agents. *Blood* 2003;101:4098–104.
- [39] Li J, Zuo L, Shen T, Xu CM, Zhang ZN. Induction of apoptosis by sodium selenite in human acute promyelocytic leukemia NB4 cells: involvement of oxidative stress and mitochondria. *J Trace Elem Med Biol* 2003;17:19–26.
- [40] Droge W. Free radicals in the physiological control of cell function. *Physiol Rev* 2002;82:47–95.
- [41] Perluigi M, De Marco F, Foppoli C, Coccia R, Blarzino C, Marcante ML, et al. Tyrosinase protects human melanocytes from ROS-generating compounds. *Biochem Biophys Res Commun* 2003;305:250–6.
- [42] Hampton MB, Fadeel B, Orrenius S. Redox regulation of the caspases during apoptosis. *Ann N Y Acad Sci* 1998;854:328–35.
- [43] Hahiwel B, Gutteridge JMC. *Free radicals in biology and medicine*. Oxford: Oxford University Press; 1999.
- [44] Davis CA, Nick HS, Agarwal A. Manganese superoxide dismutase attenuates cisplatin-induced renal injury: importance of superoxide. *J Am Soc Nephrol* 2001;12:2683–90.
- [45] Eguchi Y, Shimizu S, Tsujimoto Y. Intracellular ATP levels determine cell death fate by apoptosis or necrosis. *Cancer Res* 1997;57:1835–40.
- [46] Leist M, Single B, Castoldi AF, Kuhnle S, Nicotera P. Intracellular adenosine triphosphate (ATP) concentration: a switch in the decision between apoptosis and necrosis. *J Exp Med* 1997;185:1481–6.
- [47] Eguchi Y, Shimizu S, Tsujimoto Y. ATP-dependent steps in apoptotic signal transduction. *Cancer Res* 1999;59:2174–81.
- [48] Edinger AL, Thompson CB. Death by design: apoptosis, necrosis and autophagy. *Curr Opin Cell Biol* 2004;16:663–9.
- [49] Rodriguez-Enriquez S, He L, Lemasters JJ. Role of mitochondrial permeability transition pores in mitochondrial autophagy. *Int J Biochem Cell Biol* 2004;36:2463–72.